Adaptive Modeling, Prediction, and Tracking of Wireless Fading Channels

Abdorreza Heidari and Amir K. Khandani

Authors' names in full - Nom et prénom des auteurs	Birthdate - Date de naissance	Canadian Citizen Citoyen canadien	Landed Immigrant Immigrant reçu	Non-Canadian Étranger
Heidari, Abdorreza	February 28, 1975	☐	X	☐
Khandani, Amir, Keyvan	December 2, 1959	X	☐	☐
		☐	☐	☐

Title of publication - Titre de la publication	Publisher - Maison d'édition
Adaptive Modeling, Prediction and Tracking of Wireless Fading Channels	University of Waterloo

Where can booksellers and libraries obtain copies? Où les libraries et les bibliothèques peuvent-elles se procurer des exemplaires?		
University of Waterloo Dept. of Electrical and Computer Engineering 200 University Avenue West Waterloo, ON N2L 3G1 CANADA	**ISBN number - Numéro d'ISBN**	**Retail sale price - Prix de détail**
	Date published - Date d'édition	**Print run - Tirage** 1st run

Signature

Is distribution limited? La distribution est-elle restreinte?	☐ Yes (to whom?) Oui (à qui?) X No - Non

Date: January 8, 2007

Telephone no. - Nº de téléphone
519-885-1211

Fax no. - Nº de télécopieur
519-746-3077

Internet
www.ece.uwaterloo.ca

Heidari, Abdorreza, 1975-
Adaptive modeling, prediction, and tracking of wireless fading channels / Abdorreza Heidari and Amir K. Khandani
Waterloo, Ont. : University of Waterloo. Dept. of Electrical & Computer Engineering, [2007.]

Adaptive Modeling, Prediction, and Tracking of Wireless Fading Channels

Abdorreza Heidari and Amir K. Khandani

Coding and Signal Transmission Laboratory (www.cst.uwaterloo.ca)

Dept. of Elec. and Comp. Eng., University of Waterloo

Waterloo, ON, Canada, N2L 3G1

Tel: 519-883-3950, Fax: 519-888-4338

E-mails: {reza,khandani}@cst.uwaterloo.ca .

Abstract

A key element for many fading-compensation techniques is long-range prediction of the fading channel. A linear approach, usually used to model the time evolution of the fading process, does not perform well for long-range prediction. In this article, we propose an adaptive channel prediction algorithm using a state-space approach for the fading process based on the sum-sinusoidal model. Our simulations show that this algorithm significantly outperforms the conventional linear method, for both stationary and non-stationary fading processes, especially for long-range predictions. The self-recovering structure, as well as the reasonable and steady computational complexity, makes the proposed algorithm appealing for practical applications[1].

Index Terms

Wireless/Mobile Fading Channel, Channel Modeling, Channel Prediction, Sum-Sinusoidal model, State-Space Model, Kalman Estimation, Adaptive Filtering

I. INTRODUCTION

In this article, we address the problem of channel fading modeling and prediction. Channel fading prediction can be used to improve the performance of telecommunication systems. Having estimates of future samples of the fading coefficients enhances the performance of many tasks at the receiver and/or at the transmitter, including channel equalization, the decoding process of data symbols, antenna beamforming, and adaptive coding and modulation.

Consider a fading channel from a transmit antenna to a receive antenna. A single path flat fading is assumed for the channel. If the path delay variations are not negligible in comparison with the symbol period, the same analysis could be applied to each resolved multipath component. The channel fading coefficient h_n is zero mean (subscript n is the time index), with the variance $\sigma_h^2 = 1$. Fig. 1 shows the block diagram for prediction of a fading channel. The channel coefficients are estimated from the received signal series $\{y_n\}$, where the nature of y_n could be different depending on the application. Usually y_n is a pilot signal which is appropriately designed for channel estimation, as in 3G systems. In some applications, y_n is the modulated user data which is used by a blind channel estimation algorithm. The subject of channel fading estimation is well-established in the literature and will not be addressed here. We assume that the channel estimate $\overline{h}_n$ is shown as $\overline{h}_n = h_n + v_n$, where v_n is the estimation error modeled as a zero mean Gaussian noise [1] with the variance σ_v^2. As an indicator for the estimation quality, the observation SNR is defined as $\text{SNR}_z = \sigma_h^2/\sigma_v^2 = 1/\sigma_v^2$.

For prediction of a future sample of the channel using the past measurements, a model is needed to represent the dynamics of the channel. Having the series of the channel measurements $\{\overline{h}_n\}$, the parameters of the model are estimated or updated, and the future fading sample is predicted as shown in Fig. 1. The model selection and extraction of the
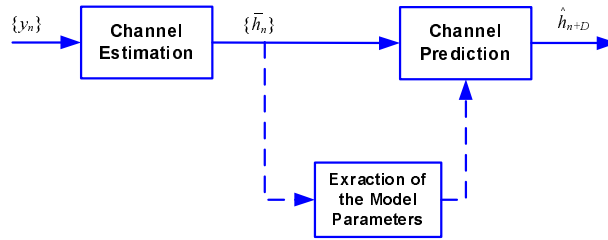
Fig. 1.   Block diagram of a channel prediction scheme

parameters, as well as the prediction algorithm, are explained in the sequel.

Many processes are represented with a linear model, i.e. an auto-regressive moving-average (ARMA) model. In this context, an approximate low-order AR model is often used as it can capture most of the fading dynamics. For example, see the MMSE linear predictor proposed in [2], and the channel tracking algorithms utilizing Kalman filter in [3] and [4]. Linear models are easy to use and have a low complexity, but they fail to show the true time behavior of a channel fading process.

A fading channel can be modeled as sum of a number of sinusoids as shown in (29). This model relies on the physical scattering mechanism [5]. The so-called sum-sinusoidal model has been used for prediction of the channel fading [6], [7], [8], [9]. In this article, we use the sum-sinusoidal model in a Kalman filtering framework as suggested in our earlier work [10]. This model is *adaptively* updated to follow the changes in the scattering environment.

Assuming a two-dimensional isotropic scattering and an omni-directional receiving antenna, it is known that the autocorrelation function of the fading process can be written as [5]

$$R_h(t, t - \tau) = \frac{E[h(t)h^*(t - \tau)]}{\sigma_h^2} = J_0(2\pi f_d \tau), \tag{1}$$

where f_d is the maximum doppler frequency, $J_0(\cdot)$ is the first-kind Bessel function of the zero order, and τ is the time difference. A Rayleigh fading process with the above

correlation property is called the Jakes fading [5]. We use a wide-sense stationary (WSS) version of the Jakes fading [11] (which uses 14 low-frequency sinusoids) to examine the performance of the underlying algorithms. We also generate a non-stationary and more realistic mobile fading using a ray-tracing approach [10], and examine the algorithms with the non-stationary fading as well.

Here is a summary of the contributions of this article:

- Linear approach (Section II):

  – A 1-step predictor is conventionally used for the linear method. Here a D-step predictor (D≥1) is presented, and the relation to the 1-step predictor is addressed.

  – A tracking algorithm for the D-step predictor is proposed.

- The proposed approach (Section III):

  – Based on the sum-sinusoidal fading model, a state-space model is proposed.

  – Using the state-space model, an adaptive Kalman algorithm is proposed. The algorithm is presented for both acquisition and tracking phases.

  – A tracking algorithm for the doppler frequencies is proposed.

  – An enhancement to the prediction part of the adaptive Kalman filter is proposed.

In the next two sections, The linear approach and the proposed approach are presented. Then, the algorithms are compared in the simulation results.

II. LINEAR APPROACH

To model a fading process, a linear model is widely used. An AR (Auto Regressive) model of order N_{AR} is recursively defined as follows

$$h_{n+1} \;=\; \sum_{i=1}^{N_{\mathrm{AR}}} a(i)\, h_{n-i+1} + \xi_{n+1} \tag{2}$$

where $\mathbf{a} = [a(1), a(2), \cdots, a(N_{\text{AR}})]^T$ is the AR coefficients vector, and ξ_{n+1} is the model error which has a zero mean.

The time evolution of an AR model can also be shown as a state-space model [3] as follows

$$\begin{cases} \mathbf{h}_n = \mathbf{B}\,\mathbf{h}_{n-1} + \mathfrak{q}_n \\ \\ z_n = \mathfrak{m}\,\mathbf{h}_n + u_n \end{cases} \tag{3}$$

where

$$\mathbf{h}_n = [h_n,\, h_{n-1},\, \cdots,\, h_{n-N_{\text{AR}}+1}]^T \tag{4}$$

is the fading regressor at time n, $\mathbf{B}$ is the transition matrix defined as

$$\mathbf{B} = \begin{pmatrix} & \mathbf{a}^T & \\ \\ \mathbf{I}_{N_{\text{AR}}-1 \times N_{\text{AR}}-1} & & \mathbf{0}_{\mathbf{N_{\text{AR}}-1 \times 1}} \end{pmatrix}, \tag{5}$$

and $\mathfrak{q}_n$ is a noise vector representing the model error. $\mathfrak{m}$ is known as the measurement matrix which is defined as

$$\mathfrak{m} = [1,\, 0,\, \cdots,\, 0]_{1 \times N_{\text{AR}}}, \tag{6}$$

u_n is the observation noise, and z_n is the system output.

It is easy to show that $\hat{\mathbf{h}}_{n+1|n} = \mathbf{B}\,\mathbf{h}_n$, where $\hat{\mathbf{h}}_{n+1|n}$ is the prediction of $\mathbf{h}_{n+1}$ given the observations up to the time n, i.e., $\hat{\mathbf{h}}_{n+1|n} = E\left[\mathbf{h}_{n+1}|z_n,\, z_{n-1}\cdots\right]$. Similarly,

$$\hat{\mathbf{h}}_{n+D|n} = \mathbf{B}^D\,\mathbf{h}_n. \tag{7}$$

Also,

$$\hat{h}_{n+D|n} = \mathfrak{m}\,\hat{\mathbf{h}}_{n+D|n} \tag{8}$$

$$= \mathfrak{m}\,\mathbf{B}^D\,\mathbf{h}_n. \tag{9}$$

A. The Linear Prediction Algorithm (LP)

Assuming an AR model of the order N_{AR}, a 1-step linear predictor is shown as follows

$$\hat{h}_{n+1} \;=\; \sum_{i=1}^{N_{\text{AR}}} a(i)\,\overline{h}_{n-i+1}. \tag{10}$$

Minimizing the mean square error (MSE), $E\left[\left|h_n - \hat{h}_n\right|^2\right]$, provides the prediction coefficients $\mathbf{a}$ via solving the Yule-Walker equations [12].

For the Jakes fading, $\mathbf{a}$ is analytically available [13]. In practice, $\mathbf{a}$ is estimated using the fading samples using one of the well-known methods such as Levinson method, Burg method, or Prony method. In a non-stationary environment, the coefficients is frequently updated to follow the model variations.

Here, the linear coefficients are estimated using a Least-Squares approach and solving the equations by the Levinson-Durbin recursion over a window length of T_{AR}. The estimates are updated every T_{AR} samples. Fig. 2 shows the flowchart of the algorithm.

1) D-step Prediction Versus 1-step Prediction: To perform a D-step prediction, the 1-step predictor could be used D times recursively. However, we are interested in a direct D-step prediction method because it is easier to analyze and also to implement. Furthermore, this is particularly helpful in the tracking mode as it is addressed in Section II-A.2. Equation (10) can be extended to provide a D-step linear predictor [13], as follows

$$\hat{h}_{n+D} \;=\; \sum_{i=1}^{N_{\text{AR}}} a^{(D)}(i)\,\overline{h}_{n-i+1}. \tag{11}$$

The superscript "(D)" indicates that the variable is related to the D-step predictor. Calculation of the coefficients of the 1-step predictor, $\mathbf{a}$, was explained before. For the D-step predictor,

$$\mathbf{a}^{(D)} = [a^{(D)}(1),\; a^{(D)}(2),\; \cdots,\; a^{(D)}(N_{\text{AR}})]^T \tag{12}$$
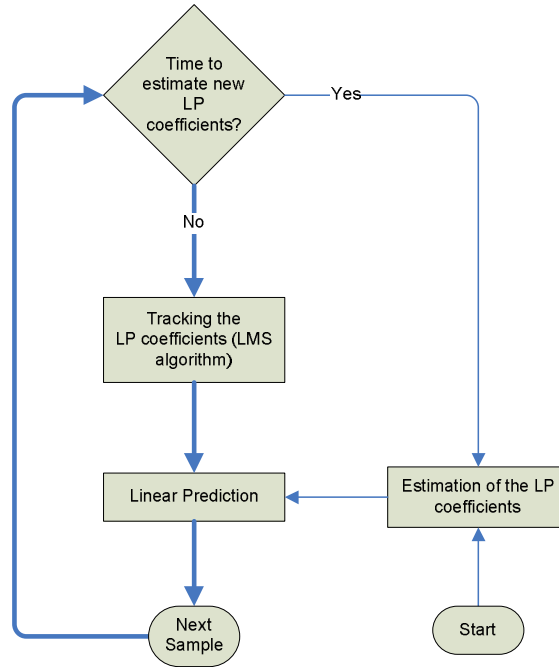
Fig. 2. Block Diagram of the Linear Prediction Algorithm (LP)

can be computed using $\mathbf{a}$. It is evident from (9) that $\mathbf{a}^{(D)} = (\mathfrak{m}\,\mathbf{B}^D)^T$, meaning $\mathbf{a}^{(D)^T}$ is the first row of $\mathbf{B}^D$. Hence, the calculation steps are as follows:

$$\mathbf{a} \to \mathbf{B} \to \mathbf{B}^D \to \mathbf{a}^{(D)} \tag{13}$$

2) Tracking: In a non-stationary environment, model in changing and the assumption of a fixed model over the observation window results in a performance degradation. A low-complexity adaptive algorithm is desired to track the changes of $\mathbf{a}_n$ over time. An LMS algorithm is used as in [14]

$$\mathbf{a}_{n+1} = \mathbf{a}_n + \mu_{\text{AR}}\,\mathbf{h}_n^H\,e_n \tag{14}$$

where $e_n = h_n - \hat{h}_n$. Note that we have added the time index n for $\mathbf{a}_n$ in the tracking mode signifying that it is changing at each time step.

As explained in Section II-A.1, $\mathbf{a}_n^{(D)}$ is calculated using $\mathbf{a}_n$, which requires the calculation of $\mathbf{B}_n^D$. In the tracking mode, this calculation is needed at each time that $\mathbf{a}_n$

is updated which imposes a high computational complexity. In the following, we propose a method to decrease the complexity.

Assume that δ_n is the increment vector

$$\mathbf{a}_{n+1} = \mathbf{a}_n + \delta_n. \tag{15}$$

This form of iteration includes many adaptive methods, most importantly LMS and RLS algorithms. From (15) and (5), we may write

$$\mathbf{B}_{n+1} = \mathbf{B}_n + \Delta_n \tag{16}$$

where

$$\Delta_n = \begin{pmatrix} \delta_n^T \\ \\ \mathbf{0}_{(\mathbf{N}_{AR}-\mathbf{1})\times\mathbf{N}_{AR}} \end{pmatrix} \tag{17}$$

Assuming a sufficiently large sampling frequency, $\mathbf{a}_n$ is slowly changing with the time index n, and δ_n has a small norm. Therefore,

$$\mathbf{B}_{n+1}^D = (\mathbf{B}_n + \Delta_n)^D \tag{18}$$

$$\cong \mathbf{B}_n^D + \sum_{i=1}^{D} \mathbf{B}_n^{i-1} \Delta_n \mathbf{B}_n^{D-i} \tag{19}$$

$$= \mathbf{B}_n^D + \Delta_n^{(D)} \tag{20}$$

where (19) is approximated by neglecting the terms in which Δ_n has a power larger than one. Therefore, we may write

$$\mathbf{a}_{n+1}^{(D)} = \mathbf{a}_n^{(D)} + \delta_n^{(D)}, \tag{21}$$

which corresponds to the operation of the first rows of the matrices in (20). Now, $\delta_n^{(D)}$ can be calculated using δ_n as follows,

$$\delta_n \to \Delta_n \to \Delta_n^{(D)} \to \delta_n^{(D)} \tag{22}$$

$$\mathbf{G}_n^{(1)} = \begin{pmatrix} 1 & 0 & 0 \\ 0 & 1 & 0 \\ 0 & 0 & 1 \end{pmatrix}, \quad \mathbf{G}_n^{(2)} = \begin{pmatrix} 2\,a_n(1) & 1 & 0 \\ a_n(2) & a_n(1) & 1 \\ a_n(3) & 0 & a_n(1) \end{pmatrix} \tag{24}$$

$$\mathbf{G}_n^{(3)} = \begin{pmatrix} 3\,a_n(1)^2 + 2\,a_n(2) & 2\,a_n(1) & 1 \\ 2\,a_n(1)\,a_n(2) + a_n(3) & 2\,a_n(2) + a_n(1)^2 & a_n(1) \\ 2\,a_n(1)\,a_n(3) & a_n(3) & a_n(1)^2 + a_n(2) \end{pmatrix} \tag{25}$$

$$\mathbf{G}_n^{(4)} = \begin{pmatrix} 4\,a_n(1)^3 + 6\,a_n(1)\,a_n(2) + 2\,a_n(3) & 3\,a_n(1)^2 + 2\,a_n(2) & 2\,a_n(1) \\ 3\,a_n(1)^2 a_n(2) + 2\,a_n(1)\,a_n(3) + 2\,a_n(2)^2 & 4\,a_n(1)\,a_n(2) + 2\,a_n(3) + a_n(1)^3 & 2\,a_n(2) + a_n(1)^2 \\ a_n(3)\left(3\,a_n(1)^2 + 2\,a_n(2)\right) & 2\,a_n(1)\,a_n(3) & 2\,a_n(3) + a_n(1)^3 + 2\,a_n(1)\,a_n(2) \end{pmatrix} \tag{26}$$

where $\delta_n^{(D)}$ is obtained from the first row of $\Delta_n^{(D)}$. It is observed from (19) that each element of $\Delta_n^{(D)}$ is a linear combination of the elements of Δ_n (or equivalently δ_n). Therefore, we can write

$$\delta_n^{(D)} = \mathbf{G}_n^{(D)}\,\delta_n \tag{23}$$

where matrix $\mathbf{G}_n^{(D)}$ is a function of the elements of $\mathbf{a}_n$.

Equations (24)-(26) show $\mathbf{G}_n^{(D)}$ for $D = 1, 2, 3, 4$, for $N_{\mathrm{AR}} = 3$. As $\mathbf{a}_n$ is slowly changing, $\mathbf{G}_n^{(D)}$ may be recalculated only in the acquisition mode. This approximation can be further simplified, if $\mathbf{G}_n^{(D)}$ is calculated for a fixed typical channel. For the channel

$\mathbf{a} = [1, 0, \cdots, 0]^T$, $\mathbf{G}_n^{(D)}$ has a simple form; for example for $N_{\mathrm{AR}} = 3$,

$$\mathbf{G}_n^{(D)} \approx \begin{pmatrix} D & D-1 & D-2 \\ & & \\ 0 & 1 & 1 \\ & & \\ 0 & 0 & 1 \end{pmatrix}. \tag{27}$$

Our simulations show that the performance does not change significantly with this approximation in a wide range of mobile speed and D.

III. THE PROPOSED APPROACH

When the receiver, the transmitter, and/or the scatterers are moving, each scattered component undergoes a doppler frequency shift given approximately by [15], [14]

$$f(k) = f_d \, \cos(\theta(k)) \tag{28}$$

where $\theta(k)$ is the incident radiowave angle of the k'th component with respect to the motion of the mobile and f_d is the maximum doppler frequency defined as $f_d = \frac{V}{C} f_c$, where f_c is the carrier frequency, V is the mobile speed and C is the speed of light. Assuming N_{sc} scatterers, the complex envelop of the flat fading signal at the receiver is

$$h(t) = \sum_{k=1}^{N_{\mathrm{sc}}} a(k) \, e^{j(\omega(k)\,t + \phi(k))} + \zeta(t) \tag{29}$$

where for the k'th scatterer, $a(k)$ is the (real) amplitude, $\phi(k)$ is the initial phase, $\omega(k) = 2\pi f(k)$, and $\zeta(t)$ is the model error. The phase $\phi(k)$ can be absorbed in the amplitude as $\alpha(k) = a(k) \, e^{j\phi(k)}$. Assuming a sampling rate of $f_s = 1/T_s$, the fading samples can be written as

$$h_n = \sum_{k=1}^{N_{\mathrm{sc}}} \alpha(k) \, e^{j\omega(k)nT_s} + \zeta_n \tag{30}$$

where $h_n = h(nT_s)$, and n is the time index. In the realistic mobile environments, there are usually a few main scatterers which construct the fading signal [16]. Note that the

Jakes model is a special case of the sum-sinusoidal model, and is mathematically valid only for a rich-scattering environment.

A. Estimation of the Model Parameters

A majority of the works on channel modeling use a statistical approach. However, the fading model (30) could be observed as a deterministic equation, and a handful of articles have used this approach to capture the behavior of the fading process, e.g., refer to [6], [7], [8], [9]. Assuming N_{sc} scatterers, there are $2\,N_{\mathrm{sc}}$ unknown parameters to be determined in the model given in (30). As a systematic solution, only $2\,N_{\mathrm{sc}}$ fading samples are required to form an equation set. Solving the equation set provides $\omega(k)$ and $\alpha(k)$, for $k = 1, \cdots, N_{\mathrm{sc}}$. As this approach uses only a few noisy measurements of the fading process, it could result in poor estimation of the parameters. Article [7] uses an improved method to find the parameters using an ESPIRIT algorithm to find the doppler frequencies, and then solving a set of linear equations by the Least-Squares method to estimate the complex amplitudes. Alternatively, article [6] uses the Root-MUSIC method to find the doppler frequencies.

To estimate the amplitudes $\alpha(k)$, the Least Squares and the Bayesian methods are used in [8] assuming that $\omega(k)$'s are known. As another solution, it assumes an AR model for each $\alpha(k)$, estimates the AR coefficients using a Modified Covariance method, and constructs a Kalman filter on the AR model to estimate the amplitudes [8].

In this paper, we propose a new approach to find the parameters. The details of the method follows.

Assuming a constant scattering model, Fourier transform of the fading signal shown in (30) is

$$H(\omega) = \sum_{k=1}^{N_{\mathrm{sc}}} \alpha(k)\, \delta(\omega - \omega(k)) + \S(\omega) \tag{31}$$

This means that different scattering components are decoupled in the frequency domain and consequently can be estimated. The Fourier analysis provides an accurate estimation of $\omega(k)$'s if they do not change significantly over the observation window. In practice, the $\omega(k)$'s change slowly with time. Therefore, a high-resolution method is required to estimate the doppler frequencies using a short window of recent measurements, as in [6], [7], [8]. Furthermore, these estimates need to be performed frequently which imposes a high computational complexity. However, this problem can be solved by an adaptive filter. We utilize a tracking loop to follow the slow variations of $\omega(k)$'s at each fading sample. Therefore, unlike the window-based methods, the doppler frequencies are up-to-date at each sample. A sudden change in the frequencies may occasionally happen, for example, if the mobile path abruptly changes. In this case, the frequencies are estimated again. Because of the nature of this approach, initial estimates of the frequencies do not need to be very accurate. Therefore, we can use a simple fourier analysis like an FFT algorithm.

As can be seen in (31), the $\alpha(k)$'s may also be estimated from the Fourier analysis. However, $\alpha(k)$'s usually change faster than $\omega(k)$'s as the mobile moves and the scattering environment changes. These changes may even be significant over a few fading samples. Therefore, the estimates of the $\alpha(k)$'s should be kept up-to-date. Knowing $\omega(k)$'s, we construct a Kalman filter based on the sum-sinusoidal model to efficiently follow the $\alpha(k)$ variations using each sample of the channel measurements. The state-space model is introduced in the next two sections.

B. The State-Space Model

A time evolution model is a useful tool for the prediction of a process. A well-known form of an evolution model known as the state-space model can be written as

$$
\begin{cases}
\mathbf{x}_n = \mathbf{A}_n \, \mathbf{x}_{n-1} + \mathbf{q}_n \\
\\
z_n = \mathbf{m}_n \, \mathbf{x}_n + v_n
\end{cases}
\tag{32}
$$

where $\mathbf{x}_n$ is an $N_{\text{ray}} \times 1$ state vector at time n, $\mathbf{A}_n$ is an $N_{\text{ray}} \times N_{\text{ray}}$ matrix which controls the transition of the state vector in time, and $\mathbf{q}_n$ is a noise vector with the covariance $\mathcal{Q}_n = E[\mathbf{q}_n \, \mathbf{q}_n^H]$, which represents the model error. The $\mathbf{m}_n$ is the measurement matrix, v_n is the observation noise, and z_n is the system output. In practical systems, $\mathbf{A}_n$, $\mathcal{Q}_n$ and $\mathbf{m}_n$ are usually constant or slowly time-varying. A well-known state-space representation of an AR model can be found in [10]. We propose a new state-space model for the mobile fading in the next section.

Considering the sum-sinusoidal process given in (30), we propose the following state-space model:

$$
\mathbf{A}_n = diag \left[e^{j\omega_n(1)\,T_s}, \; e^{j\omega_n(2)\,T_s}, \; \cdots, \; e^{j\omega_n(N_{\text{ray}})\,T_s} \right]
\tag{33}
$$

and

$$
\mathbf{m}_n = [1, \, 1, \, \cdots, \, 1]_{1 \times N_{\text{ray}}},
\tag{34}
$$

where N_{ray} is the model order which is the number of the assumed scatterers (ideally, $N_{\text{ray}} = N_{\text{sc}}$). The z_n in (32) is substituted with the available measurement of the fading sample, i.e., $z_n = \overline{h}_n$. Therefore, the state vector $\mathbf{x}_n$ consists of the complex envelops of the scattering components. A Kalman filter can utilize the state-space model to estimate the state $\mathbf{x}_n$ at each time.
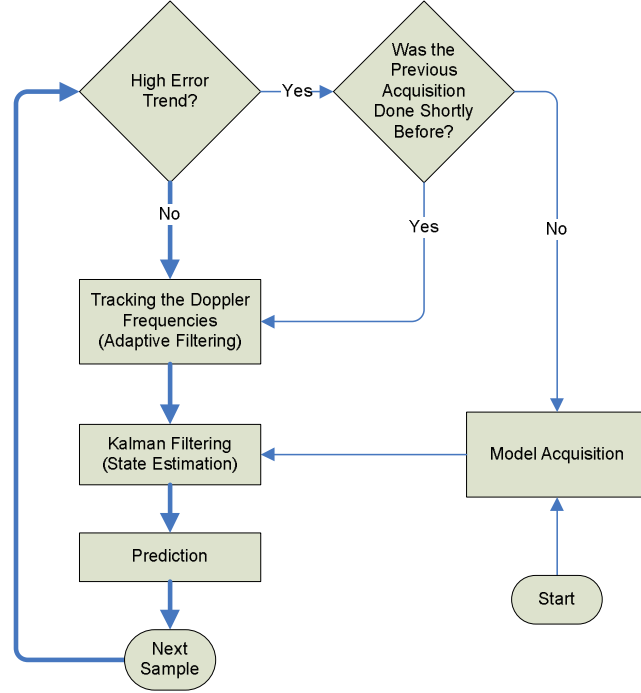
Fig. 3.   Block Diagram of Proposed Prediction Algorithm (KF)

C. The Proposed Algorithm (KF)

We propose an adaptive fading prediction algorithm here. Fig. 3 shows the flowchart of the algorithm, and a description of the main blocks follows.

1) Kalman Filtering: Kalman Filtering is now commonly used in communication systems (for example, see [3], [17], [4]). Assuming a state-space model, Kalman filter efficiently estimates the state vector $\mathbf{x}_n$ using the observation samples. The estimation of the state vector given the observations at the time n, shown as $\mathbf{x}_{n|n}$, is optimal in the MMSE sense. This state vector is used to predict the future samples of the fading signal later.

Table I shows the Kalman equation, and Table II defines the variables used in the Kalman equations. The presented Kalman filter works perfectly as long as the assumed model represented by $\mathbf{A}_n$ is valid. In the transient times when the model is changing, the Kalman filter may lose the track of the state. A threshold is imposed on the magnitude of

Prediction part:

$$\mathbf{x}_{n|n-1} \quad = \quad \mathbf{A}_n \, \mathbf{x}_{n-1|n-1} \tag{35}$$

$$\mathbf{P}_{n|n-1} \quad = \quad \mathbf{A}_n \, \mathbf{P}_{n-1|n-1} \mathbf{A}_n^T + \mathbf{Q} \tag{36}$$

Update part:

$$\mathbf{k}_n \quad = \quad \mathbf{P}_{n|n-1} \, \mathbf{m}_n^H \left(\mathbf{m}_n \, \mathbf{P}_{n|n-1} \, \mathbf{m}_n^H + \sigma_v^2 \right)^{-1} \tag{37}$$

$$\mathbf{x}_{n|n} \quad = \quad \mathbf{x}_{n|n-1} + \mathbf{k}_n \left(z_n - \mathbf{m}_n \, \mathbf{x}_{n|n-1} \right) \tag{38}$$

$$\mathbf{P}_{n|n} \quad = \quad \mathbf{P}_{n|n-1} - \mathbf{k}_n \, \mathbf{m}_n \, \mathbf{P}_{n|n-1} \tag{39}$$

TABLE I

KALMAN EQUATIONS

the error term in (38), $\epsilon_n = z_n - \mathbf{m}_n \, \mathbf{x}_{n|n-1}$, to prevent large invalid changes. Namely, if $|\epsilon_n| > T_\epsilon$ then $\epsilon_n' = T_\epsilon \, \epsilon_n / |\epsilon_n|$ is used instead. A threshold of $T_\epsilon = 4 \, \sigma_v$ is used here. To decrease the transient time, the estimates of $\alpha(k)$'s from the Fourier analysis are applied as initial values to the Kalman filter.

Fig. 4 shows a sample of the trajectories of $|x_n(k)|$'s versus n ($|x_n(k)| = |\alpha_n(k)|$).

2) Model Acquisition: The current parameters for the fading model are estimated according to Section III-A. We apply the Fourier method to estimate $\omega(k), k = 1, \cdots, N_{\text{ray}}$ using an FFT algorithm [13].

Acquisition could be done frequently to keep up-to-date with the doppler frequency

Q	The covariance matrix of the model noise
z_n	The observation sample
$\mathbf{x}_{n\|n-1}$	The *a priori* estimate of the state $\mathbf{x}_n$ (i.e., the estimation of the state at the time n given the observations upto the time $n-1$)
$\mathbf{x}_{n\|n}$	The *a posteriori* estimate of the state $\mathbf{x}_n$ (i.e., the estimation of the state at the time n given the observations upto the time n)
$\mathbf{P}_{n\|n-1}$	The covariance matrix of the *a priori* error
$\mathbf{P}_{n\|n}$	The covariance matrix of the *a posteriori* error

TABLE II

VARIABLES USED IN THE KALMAN FILTER

changes. But to decrease the required computations, it may be done only when the scattering model has significantly changed. The proposed algorithm enters the acquisition mode when the error trend exceeds a threshold as explained in Section III-C.5. Furthermore, the algorithm does not allow two consecutive acquisitions to happen close together because, after each acquisition, other blocks of the algorithm should have enough time to catch up with the new model parameters.

3) Tracking: An adaptive algorithm is used to track the fine changes of the doppler frequencies. Using a gradient-based approximation, the following LMS algorithm is applied (See Appendix IV for details)

$$w_{n+1}(k) = w_n(k) + \mu_{\mathrm{KF}} \, \Im \left[x_{n|n}^H(k) \, e_n \right]. \tag{40}$$

where $\Im$ is the imaginary operator and
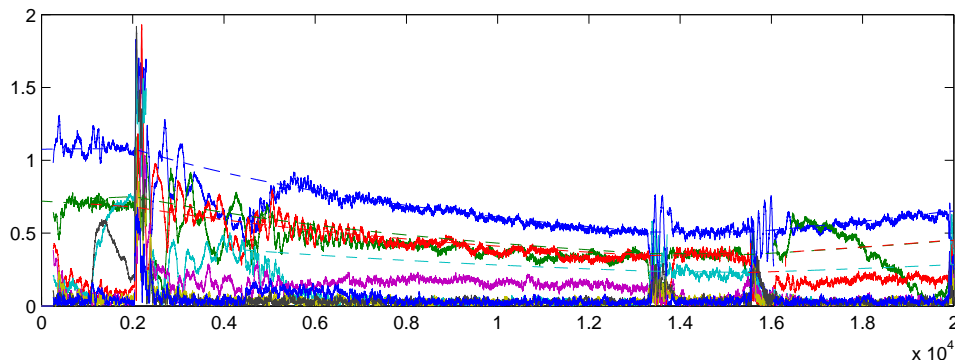
$$e_n = z_n - h_{n|n}, \tag{41}$$

Fig. 4.   A sample of the tracking capabilities of the Kalman filter for the envelopes of the scattering components

$$h_{n|n} \quad = \quad \mathbf{m}_n \, \mathbf{x}_{n|n}. \tag{42}$$

4) Prediction: Given the current state $\mathbf{x}_n$, which carries all the information about the past, the future channel state should be predicted. It has been shown [18] that given a *constant* state transition matrix $\mathbf{A}_n$, the MMSE estimate of the D-step prediction is

$$\hat{\mathbf{x}}_{n+D|n} = \mathbf{A}_n^D \, \mathbf{x}_{n|n}. \tag{43}$$

where $\hat{\mathbf{x}}_{n+D|n}$ is the estimate of the state vector at the time $n+D$, given the observations until the time n. However, the doppler frequencies slowly change, resulting in slight changes from $\mathbf{A}_{n+1}$ to $\mathbf{A}_{n+D}$. It is shown in Appendix I that considering the model changes over time, the optimal predictor is

$$\hat{\mathbf{x}}_{n+D|n} = \mathbf{A}_{n+D} \cdots \mathbf{A}_{n+2}\mathbf{A}_{n+1} \, \mathbf{x}_{n|n}. \tag{44}$$

At the time n, the matrices $\mathbf{A}_{n+2}, \cdots, \mathbf{A}_{n+D}$ are not known. However, they can be estimated by assuming the same trend for the doppler frequency changes over the next D samples. Utilizing the tracking model of (40), the following estimate is achieved (see Appendix II for the proof),

$$\mathbf{A}_{n+D} \cdots \mathbf{A}_{n+2}\mathbf{A}_{n+1} = \mathbf{A}_n^D \, diag[e^{j\frac{D(D+1)}{2} \, \delta \mathbf{w}_n T_s}], \tag{45}$$

where

$$\delta \mathbf{w}_n = \mathbf{w}_{n+1} - \mathbf{w}_n \tag{46}$$

which can be calculated using (40) or another similar algorithm.

Using the predicted state $\hat{\mathbf{x}}_{n+D|n}$, the fading sample at the time $n+D$ can be obtained as $\hat{h}_{n+D|n} = \mathbf{m}_n \hat{\mathbf{x}}_{n+D|n}$.

5) Calculation of the Error Trend: We use an exponential window for calculation of the error trend from the sample errors, as follows

$$E_{n+1} = \lambda E_n + (1 - \lambda) |e_n|^2, \tag{47}$$

where λ is the forgetting factor ($0 \ll \lambda < 1$).

Fig. 5 shows the trajectories of $|e_n|^2$ and E_n versus n, corresponding to the results shown in Fig. 4. Note that more than one acquisition may happen to follow each phase of the model change, as observed in the plots.

IV. SIMULATION RESULTS

Table III shows the simulation parameters. The two prediction algorithms (LP and KF) are compared here, with respect to the average MSE versus the prediction depth. The results are reported for various linear orders N_{AR}, and various scattering orders N_{ray}, respectively (N_{ray} is an approximation of N_{sc} in (30)). Fig. 6 shows the results for the Jakes fading for the mobile speeds of $V = 25$ and $V = 100$ kmph. It is observed that KF significantly outperforms LP if N_{ray} is large enough (here, for $N_{\text{ray}} \geq 8$), while LP fails at high prediction depths regardless of the linear order.

The Jakes fading is only valid for a rich scattering environment. Furthermore, because the Jakes fading is stationary, it can not model the changes in the scattering environment. To test the algorithms in a more realistic setting, we use a Ray-Tracing simulation environment as explained in [10]. The mobile is randomly moving vertically
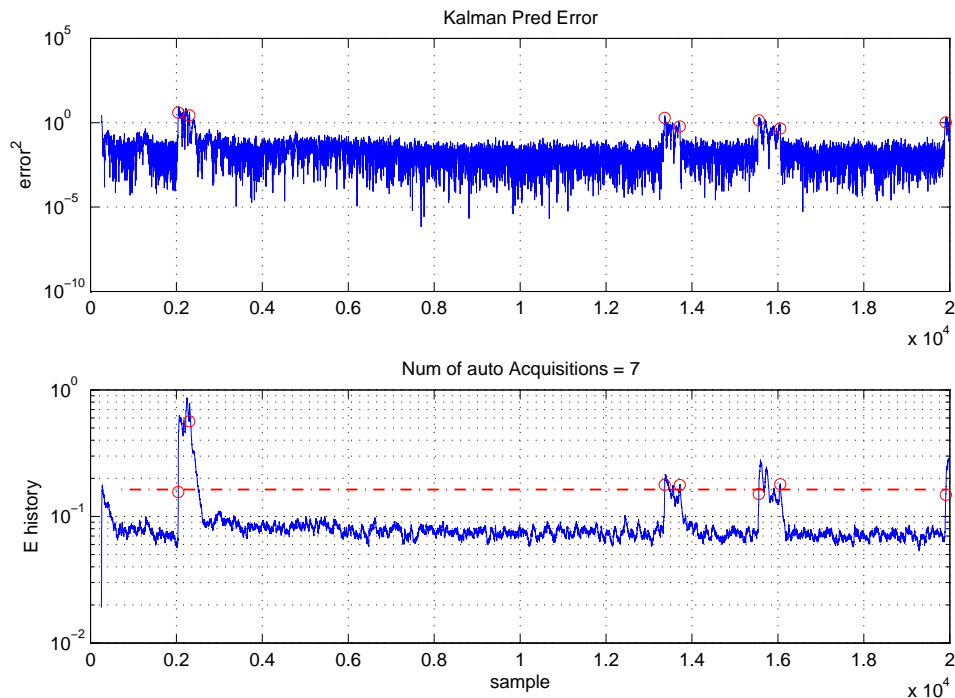
Fig. 5.   A sample of the error history for the Kalman filter

f_c	2.15 GHz
f_s	1500 Hz
SNR_z	10 dB

TABLE III

SIMULATION PARAMETERS

and horizontally in the scattering area and experiences different combinations of signal rays. At each point of the mobile path, it undergoes a different doppler frequency and a different signal power for each ray. Therefore, the generated fading, called "RT fading", can closely resemble the channel in a real mobile environment which is usually dominated by a few scatterers.

Fig. 7 shows the results for RT fading for $V = 25$ and $V = 100$ kmph. It is observed that KF can always outperform LP. For a linear predictor, the MSE is directly
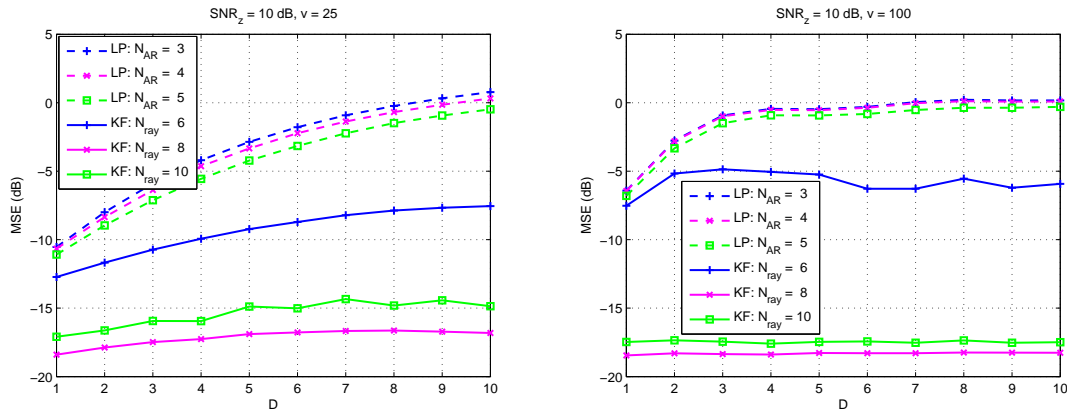
Fig. 6.   Comparison of MSE versus prediction depth for the Jakes fading at $V = 25$ and $V = 100$
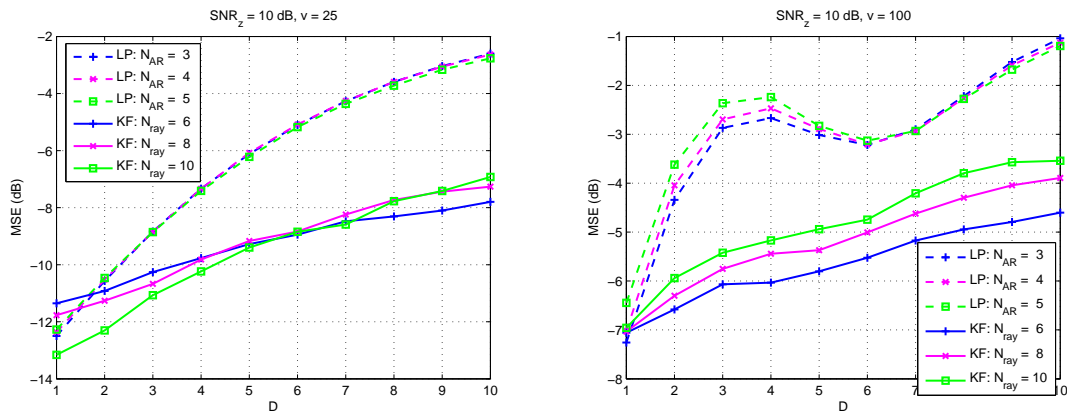

Fig. 7.   Comparison of MSE versus prediction depth for (non-stationary) RT fading at $V = 25$ and $V = 100$

related to the correlation properties of the fading, i.e., a lower correlation results in a higher MSE. The fading correlation is not monotonic, therefore the MSE versus D plot may not be increasing at high mobile speeds as observed in Fig. 7 for $V = 100$ kmph. It is also observed that increasing N_{ray} does not necessarily improve the performance. In conclusion, the simulations show that the proposed prediction algorithm can perform very well in real mobile environments, and it significantly outperforms the adaptive linear algorithm.

V. Conclusion

In this article, we propose a new method for prediction of fading channels. The doppler frequencies are estimated and updated by an acquisition-tracking method, and the amplitudes are updated by a Kalman filter. Because of the self-recovering nature of both adaptive filter and Kalman filter, the algorithm is robust to practical uncertainties such as the changes of the scattering environment, and the accuracy of the channel estimates (or observation SNR). The proposed algorithm has a reasonable complexity. Most of the existing algorithms have a window-based structure requiring frequent high-complexity computations, while the proposed method has a sample-by-sample structure resulting in a steady flow of low-complexity calculations. The simulation results show the significant advantage of the algorithm over the conventional method, especially at high mobile speeds, and low observation SNR's.

Appendices

Appendix I:

Assume the state-space model shown in (32). The state at the time $n + D$ could be written as

$$\mathbf{x}_{n+D} \quad = \quad \mathbf{A}_{n+D}\,\mathbf{x}_{n+D-1} + \mathbf{q}_{n+D} \tag{48}$$

$$= \quad \mathbf{A}_{n+D}\left(\mathbf{A}_{n+D-1}\,\mathbf{x}_{n+D-2} + \mathbf{q}_{n+D-1}\right) + \mathbf{q}_{n+D} \tag{49}$$

$$= \quad \mathbf{A}_{n+D}\mathbf{A}_{n+D-1}\mathbf{x}_{n+D-2} + \mathbf{A}_{n+D}\mathbf{q}_{n+D-1} + \mathbf{q}_{n+D} \tag{50}$$

and so on until

$$\mathbf{x}_{n+D} \quad = \quad \mathbf{A}_{n+D}\mathbf{A}_{n+D-1}\cdots\mathbf{A}_{n+1}\mathbf{x}_n +$$

$$\mathbf{A}_{n+D}\mathbf{A}_{n+D-1}\cdots\mathbf{A}_{n+2}\mathbf{q}_{n+1} + \cdots$$

$$+\mathbf{A}_{n+D}\mathbf{q}_{n+D-1} + \mathbf{q}_{n+D} \tag{51}$$

Hence, for prediction of $\mathbf{x}_{n+D}$ given the available observation data up to the time n, from (51) it can be written as

$$
\hat{\mathbf{x}}_{n+D|n} \;=\; E\left[\mathbf{x}_{n+D}|\underline{z}_n\right] \tag{52}
$$

$$
=\; \mathbf{A}_{n+D}\mathbf{A}_{n+D-1}\cdots\mathbf{A}_{n+1}E\left[\mathbf{x}_n|\underline{z}_n\right] +
$$

$$
0 + \cdots + 0 + 0 \tag{53}
$$

$$
=\; \mathbf{A}_{n+D}\mathbf{A}_{n+D-1}\cdots\mathbf{A}_{n+1}\,\mathbf{x}_{n|n} \tag{54}
$$

using the fact that $E[\mathbf{q}_i|\underline{z}_n]=0,\ i>n$.

Finally, the fading sample at the time $n+D$ can be predicted as

$$
\hat{h}_{n+D|n} \;=\; E\left[h_{n+D}|\underline{z}_n\right] \tag{55}
$$

$$
=\; E\left[\mathbf{m}_{n+D}\,\mathbf{x}_{n+D} + v_{n+D}|\underline{z}_n\right] \tag{56}
$$

$$
=\; \mathbf{m}_{n+D}\,\hat{\mathbf{x}}_{n+D|n} \tag{57}
$$

$$
=\; \mathbf{m}_{n+D}\,\mathbf{A}_{n+D}\mathbf{A}_{n+D-1}\cdots\mathbf{A}_{n+1}\,\mathbf{x}_{n|n}. \tag{58}
$$

Appendix II:

Consider the proposed state-space model described in Section III-B. Implementing (58), it can be written

$$
\mathbf{A}_{n+D}\cdots\mathbf{A}_{n+1} = diag\left[e^{j\{\omega_{n+D}(1)+\cdots+\omega_{n+1}(1)\}T_s},\ \ldots,\ e^{j\{\omega_{n+D}(N_{\mathrm{ray}})+\cdots+\omega_{n+1}(N_{\mathrm{ray}})\}T_s}\right] \tag{59}
$$

Assume the same trend for the doppler frequency changes from the time n to $n+D$, i.e.,

$$
\mathbf{w}_{n+d} \cong \mathbf{w}_n + d\,\delta\mathbf{w}_n, \quad d = 1,2,\cdots,D. \tag{60}
$$

where $\delta\mathbf{w}_n = \mathbf{w}_{n+1} - \mathbf{w}_n$. Consequently,

$$
\mathbf{A}_{n+D}\cdots\mathbf{A}_{n+1} \;=\; diag\left[e^{j\{D\,\omega_n(1)+(D+\cdots+2+1)\,\delta\omega_n(1)\}T_s},\ \ldots,\ e^{j\{D\,\omega_n(N_{\mathrm{ray}})+(D+\cdots+2+1)\,\delta\omega_n(N_{\mathrm{ray}})\}T_s}\right] \tag{61}
$$

$$
=\; \mathbf{A}_n^D\,diag\left[e^{j\frac{D(D+1)}{2}\,\delta\mathbf{w}_n T_s}\right]. \tag{62}
$$

Appendix III: Model Extension

We provided a state-space model for a single-path SISO channel in Section III-B. To extend the model to MIMO and/or multipath channels, the same approach can be used. Assume there is a total of N_{ch} different channels, where each one uses N_{ray} sinusoids. Furthermore, assume that each channel has N_{mp} resolvable multipath. The model can be shown as follows,

$$
\begin{cases}
\mathbf{X}_n = \mathbf{A}_n\,\mathbf{X}_{n-1} + \mathbf{Q}_n \\[2em]
\mathbf{Z}_n = \mathbf{M}_n\,\mathbf{X}_n + \mathbf{V}_n
\end{cases}
\tag{63}
$$

Each variable plays the same role as in (32). $\mathbf{X}_n$ is a $N_{\mathrm{ch}}N_{\mathrm{ray}} \times N_{\mathrm{mp}}$ matrix which is constructed by stacking the state vectors of different channels and different multipath components as follows

$$
\mathbf{X}_n =
\begin{pmatrix}
\mathbf{x}_n(1,1) & \mathbf{x}_n(1,2) & \cdots & \mathbf{x}_n(1,N_{\mathrm{mp}}) \\[1em]
\mathbf{x}_n(2,1) & \mathbf{x}_n(2,2) & \cdots & \mathbf{x}_n(2,N_{\mathrm{mp}}) \\[1em]
\vdots & \vdots & & \vdots \\[1em]
\mathbf{x}_n(N_{\mathrm{ch}},1) & \mathbf{x}_n(N_{\mathrm{ch}},2) & \cdots & \mathbf{x}_n(N_{\mathrm{ch}},N_{\mathrm{mp}})
\end{pmatrix}
\tag{64}
$$

where $\mathbf{x}_n(i,j)$ is the $N_{\mathrm{ray}} \times 1$ state vector of the j-th multipath of the i-th channel. $\mathbf{A}_n$ is a square matrix with $N_{\mathrm{ch}}N_{\mathrm{ray}}$ diagonal elements containing the doppler frequencies, $\mathbf{Z}_n$ and $\mathbf{V}_n$ are $N_{\mathrm{ch}} \times N_{\mathrm{mp}}$ matrices which contain the observation and the observation noise for each channel at time n, respectively. $\mathbf{M}_n$ is a $N_{\mathrm{ch}} \times N_{\mathrm{ch}}N_{\mathrm{ray}}$ matrix as depicted

in the following,

$$\mathbf{M}_n = \begin{pmatrix} \mathbf{1} & & & \\ & \mathbf{1} & & \\ & & \ddots & \\ & & & \mathbf{1} \end{pmatrix} \tag{65}$$

containing N_{ch} "$\mathbf{1}$"-vectors defined as

$$\mathbf{1} = [1,\ 1,\ \cdots,\ 1]_{1 \times N_{\mathrm{ray}}} \tag{66}$$

Appendix IV: Tracking Algorithm for the Doppler Frequencies

Considering the definition of $\mathbf{x}_n$ in (32), from (30) it can be written

$$\hat{h}_n \;=\; \sum_{k=1}^{N_{\mathrm{sc}}} x_{n-1}(k)\, e^{j\omega_n(k)T_s} \tag{67}$$

where the phase-shifts of the sinusoidal terms up to the time $n-1$ are absorbed in $x_{n-1}(k)$. Assume the cost function

$$C_n \;=\; E\left[\left|h_n - \hat{h}_n\right|^2\right] \tag{68}$$

$$\;=\; E\left[|e_n|^2\right], \tag{69}$$

where

$$e_n \;=\; h_n - \hat{h}_n. \tag{70}$$

An LMS tracking algorithm can be implemented as

$$w_{n+1}(k) = w_n(k) - \mu_0\, \frac{\partial C_n}{\partial w_n(k)}. \tag{71}$$

We can write

$$
\begin{aligned}
\frac{\partial C_n}{\partial w_n(k)} &\approx \frac{\partial |e_n|^2}{\partial w_n(k)} & (72) \\
&= \frac{\partial (e_n^H e_n)}{\partial w_n(k)} & (73) \\
&= 2\,\Re\left[(-j\,T_s\, x_{n-1}(k)\, e^{j\omega_n(k)T_s})^H\, e_n \right] & (74) \\
&= 2\,\Re\left[(-j\,T_s\, x_n(k))^H\, e_n \right] & (75) \\
&= 2\,\Re\left[j\,T_s\, x_n^H(k)\, e_n \right] & (76) \\
&= -2\,T_s\,\Im\left[x_n^H(k)\, e_n \right] & (77)
\end{aligned}
$$

where $\Re$ and $\Im$ are the real and imaginary operators, respectively. Therefore, the LMS algorithm has the following neat structure

$$
w_{n+1}(k) = w_n(k) + \mu\,\Im\left[x_n^H(k)\, e_n \right], \tag{78}
$$

where $\mu = 2\,T_s\,\mu_0$ is the step size.

REFERENCES

[1] T. Svantesson and A.L. Swindlehurst, "A Performance Bound for Prediction of MIMO Channels," *IEEE Signal Processing Magazine*, pp. 520–529, Feb. 2006.

[2] R.J. Lyman, "Optimal Mean-Square Prediction of the Mobile-Radio Fading Envelope," *IEEE Transactions on Signal Processing*, pp. 819–824, Mar. 2003.

[3] C. Komninakis, C. Fragouli, A.H. Sayed, and R.D. Wesel, "Multi-Input Multi-Output Fading Channel Tracking and Equalization Using Kalman Estimation," *IEEE Transactions on Signal Processing*, pp. 1065–1076, May 2002.

[4] M. Yan and B. D. Rao, "Performance of an Array Receiver with a Kalman Channel Predictor for Fast Rayleigh Flat Fading Environments," *IEEE Journal on selected Areas in Communications*, June 2001.

[5] W. C. Jakes, Ed., *Microwave Mobile Communications*. New York: IEEE Press, 1974.

[6] J.K. Hwang and J.H Winters, "Sinusoidal Modeling and Prediction of Fast Fading Processes," *IEEE Global Telecommunications Conference (GLOBECOM'98)*, pp. 892–897, Nov. 1998.

[7] J.B. Andersen, J. Jensen, S.H. Jensen, and F. Frederiksen, "Prediction of Future Fading Based on Past Measurements," *IEEE 50th Vehicular Technology Conference (VTC'Fall)*, pp. 151–155, Sept. 1999.

[8] Y. Liu and D. Pang, "Using the Kalman Filter for Long Range Channel Prediction," Master's thesis, Department of Signals and Systems, Chalmers University of Technology, Goteborg, Sweden, Feb. 2005.

[9] M. Chen, M. Viberg, and T. Ekman, "Two New Approaches to Channel Prediction Based on Sinusoidal Modelling," *13th IEEE/SP Workshop on Statistical Signal Processing*, pp. 697–700, July 2005.

[10] A. Heidari, A. K. Khandani, and D. McAvoy, "Channel Prediction for 3G Communication Systems," tech. rep., Bell Mobility, Aug. 2004. Available at `http://cst.uwaterloo.ca/~reza`.

[11] M. F. Pop and C. Beauliu, "Limitations of Sum-of-Sinusoids Fading Channel Simulators," *IEEE Trans. on Communications*, pp. 699–708, Apr. 2001.

[12] A. Papulis, *Probability, Random Variables, and Stochastic Processes*. McGraw-Hill, 1984.

[13] A. Heidari, D. McAvoy, and A.K. Khandani, "Adaptive Long-Range Prediction of Mobile Fading," *The 23rd Biennial Symposium on Communication, Queens University, Kingston, Ontario, Canada*, pp. 219–222, May 2006.

[14] A. Duel-Hallen and S. Hu, H. Hallen, "Long Range Prediction of Fading Signals: Enabling Adaptive Transmission for Mobile Radio Channels," *IEEE Signal Processing Magazine*, May 2000.

[15] T. S. Rappaport, *Wireless Communications: Principles and Practice*. Prentice-Hall, 1996.

[16] T. Eyceoz, A. Duel-Hallen, and H. Hallen, "Deterministic Channel Modeling and Long Range Prediction of Fast Fading Mobile Radio Channels," *IEEE Communications Letters*, Sept. 1998.

[17] H. Gerlach et al., "Joint Kalman Channel Estimation and Equalization for the UMTS FDD Downlink," *IEEE 58th Vehicular Technology Conference (VTC'Fall)*, pp. 1263–1267, Oct. 2003.

[18] G. Janacek and L. Swift, *Time Series: Forecasting, Simulation, Applications*. Prentice Hall, 1993.